ADVANCED FUNCTIONAL MATERIALS
www.afm-journal.de

Materials Views
www.MaterialsViews.com

Measuring Reduced C_{60} Diffusion in Crosslinked Polymer Films by Optical Spectroscopy

*Florian Fischer, Tobias Hahn, Heinz Bässler, Irene Bauer, Peter Strohriegl, and Anna Köhler**

The diffusion of fullerenes such as C_{60} and PCBM in organic semiconductors is a key factor in controlling the efficiency of organic solar cells, though it is challenging to measure and to control. A simple optical method based on photoluminescence quenching is developed to assess the diffusion of a quencher molecule such as C_{60} through a semiconducting polymer film, in this case made with the polymer polyfluorene. When the mobility of the polymer chains is reduced by chemical crosslinking, the diffusion coefficient of C_{60} can be reduced by up to three orders of magnitude.

1. Introduction

Due to their high electron affinity C_{60} and its derivatives, such as PCBM, are prototypical electron acceptors used in organic solar cells in which conjugated polymers are employed as electron donors. Usually the active layer is a bulk donor–acceptor heterojunction that can be prepared by simple spin-coating. Due to the intermixing of donor and acceptor, all optical excitations can be harvested by exciton diffusion towards the internal donor–acceptor interface. It is commonly assumed that in course of film deposition the fullerene forms domains whose size and structure depend on way how the solvent used in film formation is evaporated and on film annealing.[1] These processes are controlled by the diffusion of the fullerene.[1–5] Alternatively, organic solar cells can also be fabricated in the form of donor–acceptor bilayers. The disadvantage of such bilayer diodes is that only light absorbed close to the donor–acceptor interface can contribute to the photogeneration of charges. The layer thickness of this interface corresponds to the exciton diffusion length, which is typically about 5–10 nm.[6] The advantage of a bilayer structure is, however, that the transport paths of the generated electrons and holes are separated because they are confined to the donor and acceptor layers, respectively. This eliminates bimolecular charge recombination except within a thin interfacial layer which greatly simplifies the analysis of photocurrent data, provided that the donor–acceptor interface is sharp.[7] donor–acceptor bilayers can be made by spin coating using orthogonal solvents to prevent intermixing or by vapor phase deposition of the acceptor onto the donor film. To estimate whether or not the interface formed is abrupt requires knowledge on how rapidly C_{60} diffuses within the polymer film. Even though a detailed understanding on the diffusion properties of acceptor molecules such as C_{60} is essential to analyze bilayer cells, to optimize bulk heterojunction cells or to even fabricate cells with graded donor–acceptor interfaces, only limited information is available on the diffusion of C_{60}, and even less is known about ways to control and to reduce its diffusion.[3–5]

Measurements of the diffusion of molecules through a polymer film can be experimentally demanding. They often probe the motion of a tracer molecule on a microscopic rather than a macroscopic scale in order to monitor molecular motion near the glass transition. Examples are forced Rayleigh scattering or fluorescence correlation spectroscopy.[8] Secondary ion mass spectroscopy on isotopically labeled diffusion particles allows monitoring particle diffusion on a macroscopic scale.[3,4] While this method has been applied successfully to PCBM, it is experimentally demanding and it is limited to compounds that can be deuterated easily. For example, it cannot be applied to bare C_{60} because deuteration is not possible. In order to circumvent this limitation we developed an optical technique that is derived from studies of charge transport in an organic semiconductor and that is known as the time-of-flight (TOF) technique.[9] In a conventional TOF experiment, charge carriers are injected from one electrode—either optically or electrically—and move towards an exit electrode. The associated time-dependent conductivity is monitored, with a drop in conductivity indicating the arrival of the charges at the exit electrode. The arrival time then gives a measure for the carrier mobility.

One can adapt this technique to measure the diffusion of neutral C_{60} molecules or any other acceptor molecule by replacing the exit electrode with a fluorescent sensing layer. For this, a quartz substrate carrying a thin layer of a fluorescence

F. Fischer, T. Hahn, Prof. H. Bässler, I. Bauer, Prof. P. Strohriegl, Prof. A. Köhler
Bayreuth Institute of Macromolecular Science
University of Bayreuth
95440 Bayreuth, Germany
E-mail: anna.koehler@uni-bayreuth.de
F. Fischer, T. Hahn, I. Bauer, Prof. A. Köhler
Experimental Physics II
University of Bayreuth
95440 Bayreuth, Germany
Prof. P. Strohriegl
Macromolecular Chemistry I
University of Bayreuth
95440 Bayreuth, Germany

DOI: 10.1002/adfm.201401153

probe is covered with a layer of the material to be investigated, the "transport material". Finally a thin layer of C_{60} is deposited on top of the transport layer. When C_{60} molecules are "injected" to the transport layer by a sudden increase in temperature they diffuse towards the sensing layer and will eventually quench the sensor's fluorescence because C_{60} acts as a sink for optically excited sensor excitons due to transfer of the exited electron of the chromophore. The drop in the fluorescence of the sensor layer observed at a certain time is therefore a measure of the time required for the C_{60} to traverse the transport layer. To suppress the diffusion of the C_{60} through the transport material, in our case a polyfluorene polymer, it is necessary to reduce the mobility of the polymer chain. For this, we have incorporated a well-controlled amount of acrylate moieties into the side-chain of the polyfluorene that crosslink with adjacent moieties upon illumination with UV light. The observation of an increased arrival time of the C_{60} in a transport layer of the crosslinked polyfluorene indicates that the resulting network of polymer chains reduces the diffusivity of the C_{60} dramatically.

2. Results and Discussion

The experimental approach is detailed in **Figure 1**. The condition that such an experiment can work is that the incident light must only excite the sensor layer rather the transport layer. In the present case this is realized by combining polyfluorene (PF2/6) as a transport layer with a 15–17 nm thick MEH-PPV film as a sensing layer. PF2/6 absorbs in the ultraviolet spectral range from about 400 nm to shorter wavelengths while MEH-PPV can already be excited at longer wavelength down to the red spectral range. The thickness of the transport layer ranged from 0.4 μm to 4.2 μm. A 30 nm thick C_{60} layer is vapor deposited onto one half of the transport layer using a shadow mask. The C_{60}-free cell compartment serves as a reference (control) cell. The sensor layer is excited by a diode laser once in the probe area and once in the control area, and the photoluminescence of the MEH-PPV sensor in each area is detected with a CCD camera using fiber optics. Due care was taken to ensure that incident light intensities impinging on both probe and control sample areas are equal. This is illustrated in Figure 1a. The emissions from the probe area and the reference area have been recorded always immediately after each other for each data point using a shutter arrangement in the laser beam. Normalizing the emission coming from the probe cell compartment to that of the reference cell compartment provides, therefore, a measure for the quenching of sensor singlet excitons due to C_{60} molecules arriving at the sensor surface. The cells have always been measured immediately after fabrication.

Within the time-frame of the experiment, we observe no change in the sensor emission over time when the probe and reference area are compared at room temperature (Figure 1a). However, when the sample was heated to above room temperature, a distinct, sudden drop in sensor emission can be seen in the probe area at some time after the increase in temperature (Figure 1b). This is detailed in Figure 1c, with the temperature ramp indicated in the upper part of Figure 1c and the fluorescence intensity from the probe area displayed by the blue circles. The fluorescence in the control area decreases only marginally after heating as indicated by the black triangles. The red, solid curve is the time dependence of the sensor fluorescence of the presence of a C_{60} layer on top of the transport layer, normalized to the fluorescence in the absence of C_{60}. One notices that there is a minor increase of the sensor emission once the sample temperature is equilibrated. The likely reason is that sample heating reduces somewhat the internal reflection of the incident light due to smoothing of the interface between C_{60} and the transport layer, or between transport and sensing layer. After the initial heating step the sensor emission is first constant until it features a kink at a certain time, designated as the arrival time τ_{arr}. This is an indication that a sufficient number of C_{60} molecules reach the sensing layer so that its fluorescence becomes quenched. This is reminiscent of the kink observed in a time of flight signal in a transient photoconductivity experiment noting, however, that in the electrical case there is a superimposed drift current that is absent when neutral molecules diffuse across a transport layer. As expected, τ_{arr} decreases with increasing temperature (vide infra).

Diffusion theory predicts that the diffusion length L of particles is related to the diffusion coefficient and the time via

$$L = \sqrt{ZDt} \tag{1}$$

with Z = 6, 4, or 2 for three-, two-, or one-dimensional diffusion, respectively.[10] Since in this experiment the diffusion length is identical with the sample thickness one would expect that the arrival time τ_{arr} should scale with L^2/D. As can be seen in **Figure 2**, however, this is only fulfilled for PF2/6 films that are thicker than 1 μm. For thinner samples the arrival time is—within the experimental uncertainty—independent of layer thickness. The data pertaining to the crosslinked derivative PF2/6-A-75:25, also shown in Figure 2, shall be discussed further below. We shall first focus on understanding the diffusion in common, non crosslinked PF2/6. Obviously, in thin PF2/6 films the arrival time of C_{60} is not controlled by the time needed for C_{60} molecules to diffuse from the "injection" layer through the transport layer to the sensing layer. Since that time decreases by a factor of 50 upon increasing the sample temperature from 353 K to 433 K it cannot be associated with the equilibration time of the sample after the temperature jump (as the time for the sample to equilibrate should increase with increasing temperature rather than decrease). The constant arrival time for thin films must either be due to temperature activated detachment of C_{60} molecules from the "injection" layer or to their incorporation into the sensor layer. Although C_{60} transport through the polymer is diffusion-controlled, the arrival time in films thinner than 1 μm is determined by other processes. It turns out that in both cases, that is, for thin and for thick samples, the reciprocal arrival time features an Arrhenius-type of temperature dependence indicating that both, the diffusion of C_{60} through the transport layer as well as the injection or incorporation of C_{60} are thermally activated rate processes. **Figure 3** shows data for the temperature dependence of the reciprocal arrival times for a 420 nm and a 700 nm PF2/6 film. Within experimental uncertainty the results are identical for both thicknesses and yield an activation energy of 0.93 ± 0.08 eV. In contrast, the activation energy for the

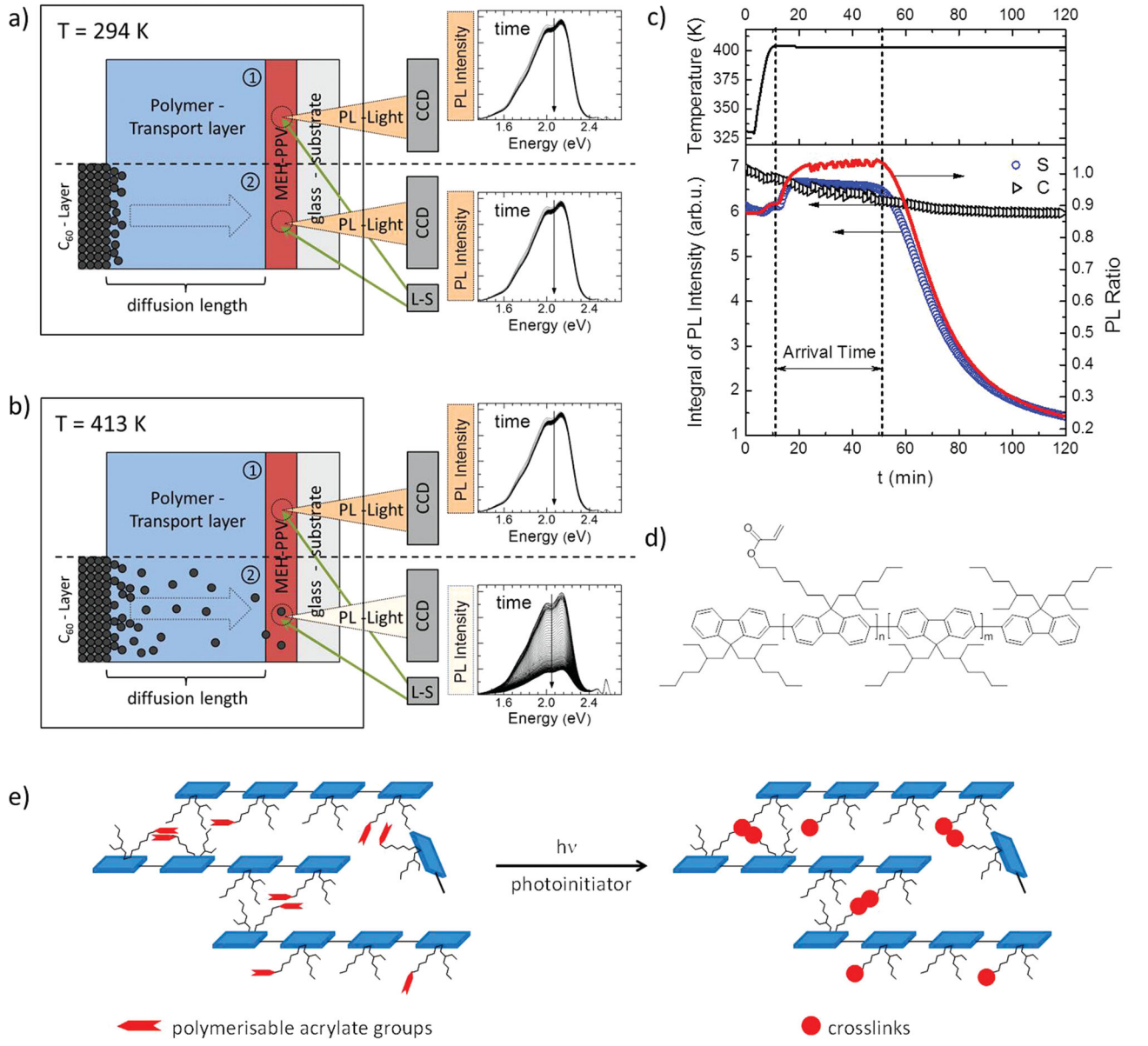

Figure 1. Illustration of the experimental procedure. a) In the control cell (1) and the sample cell (2) the fluorescence of the MEH-PPV sensor layer, excited by a diode laser-shutter unit (L-S) (485 nm), is separately recorded by a CCD camera. At room temperature the cw-fluorescence intensity is virtually constant with time. b,c) After heating up the sample within a time interval of 5–10 min to a variable operation temperature, C_{60} molecules begin to diffuse. While in the control cell the sensor fluorescence decreases only marginally (black triangles), it features a kink in the sample cell at a time (blue circles). This kink will be designated as the arrival time of the C_{60} molecules. The red solid line gives the temporal evolution of the sensor fluorescence in the probe cell normalized to that of the control cell. d) Chemical structure of PF2/6-A-n:m, a polyfluorene containing n crosslinkable repeat units with acrylate moieties. e) Illustration of the crosslinking-process.

reciprocal arrival in a 2700 nm thick PF2/6 film is 0.65 ± 0.05 eV. It must reflect the thermally activated diffusion of C_{60} through the film.

Analysis of the above C_{60} diffusion experiments requires more detailed information on the arrival time. The excitons in the sensor layer are quenched when a sufficient number of C_{60} molecules have migrated through the PF2/6 polymer film, accumulated at the interface and subsequently dope the sensor layer. This quenching process involves long range diffusion of a singlet exciton in the sensitizing MEH-PPV layer and short range electron transfer from the excited singlet state of MEH-PPV to C_{60}. It can be treated in the concept of random walk of excitons in an organic solid containing a fractional concentration c of traps.[11] If k_f is the rate constant for fluorescence decay of the undoped host and ν the rate constant of exciton hopping towards traps, the fluorescence yield is

$$\phi = \frac{k_f}{k_f + \nu c} = \left(1 + \frac{\nu}{k_f} c\right)^{-1} \quad (2)$$

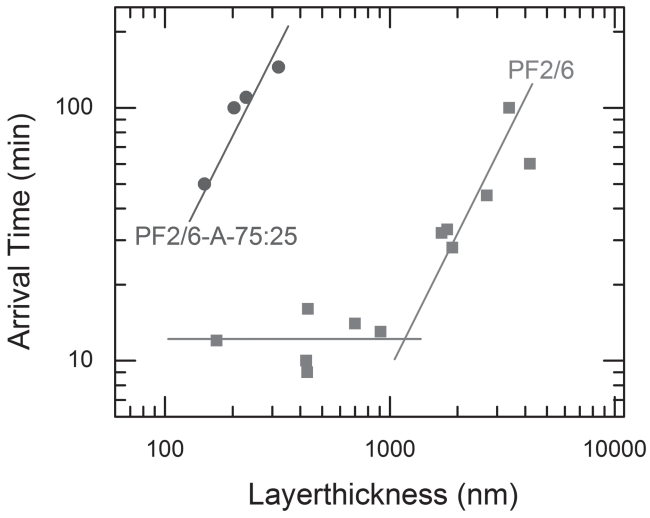

Figure 2. Arrival time of C_{60} molecules as a function of the thickness of the polymer transport layer for PF2/6 and its crosslinked derivative PF2/6-A-75:25. $T = 415$ K.

The ratio v/k_f is a measure of the number of jumps an exciton executes before it is captured by a trap, for example, by electron transfer to C_{60}. Studies of fluorescence quenching on a PPV derivative doped with trifluorenone[12] and PCPDTBT doped with C_{60}[13] show that in conjugated polymers v/k_f is about 10^3, indicating that 0.1% of traps is sufficient to reduce the fluorescence by 50%. We make the plausible assumption that C_{60} molecules that arrive at the sensor layer will subsequently diffuse into that layer and establish a homogeneous doping profile. Suppose that a monolayer of C_{60} molecules with area density of N_0 = (a^2 per unit area), where a is the lattice constant, is incorporated in the sensor layer of thickness d. It generates a concentration $1/a^2d$ of quenchers per unit volume. This is equivalent to a relative quencher concentration of a/d. According to Equation 2 this should reduce the fluorescence yield to $\varphi = (1 + f)^{-1}$ where $f = va/k_fd$. For $v/k_f = 10^3$, $a = 10^{-7}$ cm and $d = 1.6 \times 10^{-5}$ cm this yields $f = 63$. Now consider how the concentration of C_{60} inside the sensor layer evolves with time. Solving the diffusion equation in one dimension under the constraint that at $t = 0$ the concentration of the sensor interface is zero, predicts that the relative number of particles, $p = n/n_0$, to that diffused across the transport layer with thickness L after a time t' is

$$p(t') = 1 - \mathrm{erf}\left(L\left(2\sqrt{Dt'}\right)^{-1}\right) \quad (3)$$

The quenching efficiency should follow

$$\phi(t) = \left(1 + f\,p(t)\right)^{-1} \quad (4)$$

presuming that the rate-limiting step is the arrival time of C_{60} at the interface rather than the subsequent motion inside the sensor layer.

Figure 4 shows that the experimentally measured arrival signal for 1.9 µm thick PF2/6 film at 413 K can be perfectly fitted by Equation 3,4 using a diffusion coefficient

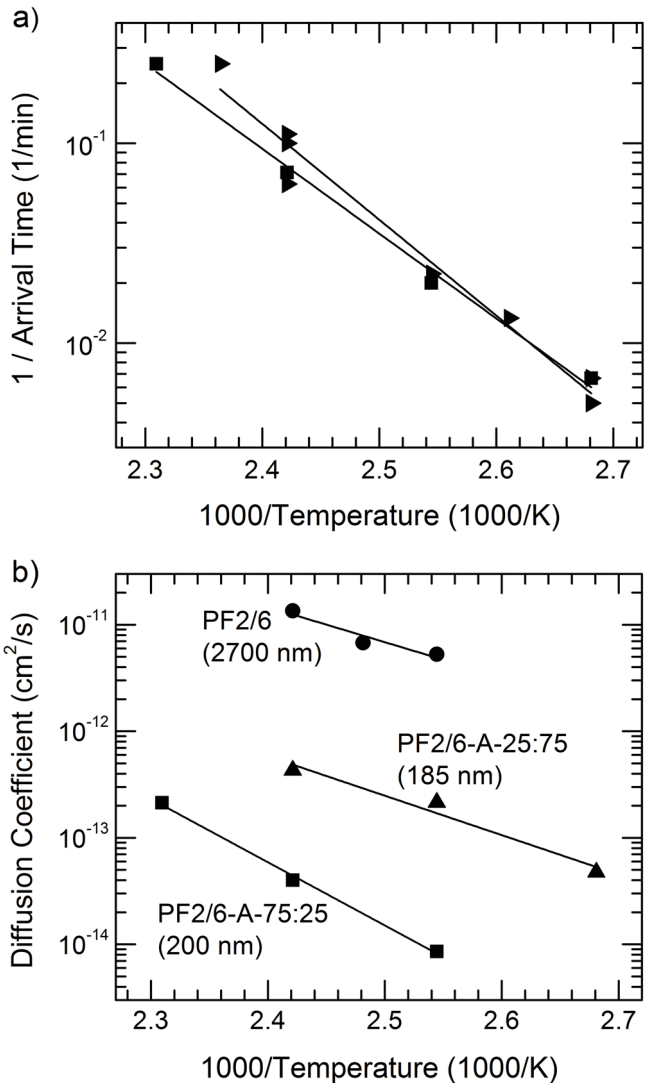

Figure 3. a) Arrhenius plot of the reciprocal arrival times of C_{60} in a PF2/6 transport layer for films of 420 nm (triangles) and 700 nm (squares) thickness, i.e., for the injection-limited regime. b) Arrhenius plot of the diffusion coefficients for films of PF2/6, PF2/6-A-25:75, and of PF2/6-A-75:25 with thicknesses as indicated in the figure, which pertain to the diffusion-limited regime for the respective materials.

$D = 1.8 \times 10^{-11}$ cm^2 s^{-1} and $f = 59$ provided that the time axis is rescaled to $t' = t = t_0$ where $t_0 = 13$ min. The arrival signal for a 3.4 µm thick PF2/6 recorded at the same temperature can be fitted with same parameters except that the value of the diffusion coefficient is by a factor of 1.8 smaller. This is likely due to uncontrollable differences in film preparation. Considering the uncertainties regarding the input parameters the agreement between experiment and theory is better than expected. In any case the perfect match between theory and experiment supports the validity of this data analysis. The rescaling of the time axis by $t_0 = 13$ min is readily accounted for the additional time required for the diffusion of C_{60} from the sensor interface into the bulk of the sensor layer. It turns out that that this time agrees with the C_{60} arrival time in thinner PF2/6 films. This suggests that t_0 is controlled by the diffusion time within the

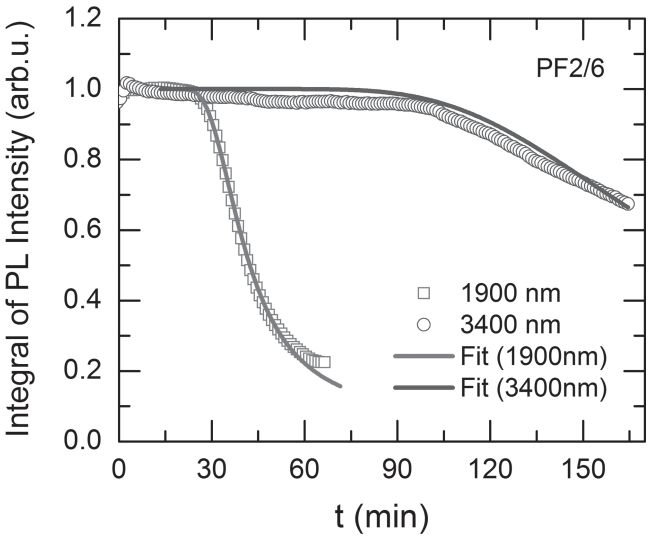

Figure 4. The temporal evolution of the sensor fluorescence in the probe cell normalized to that of the control cell for a 1900 nm thick PF2/6 layer (red squares) and for a 3400 nm thick PF2/6 layer (blue circles). The red solid line gives the fit for the 1900 nm thick PF2/6 probe and the blue solid line the fit for the 3400 nm thick PF2/6 probe. The fit-function and parameters are given in the text.

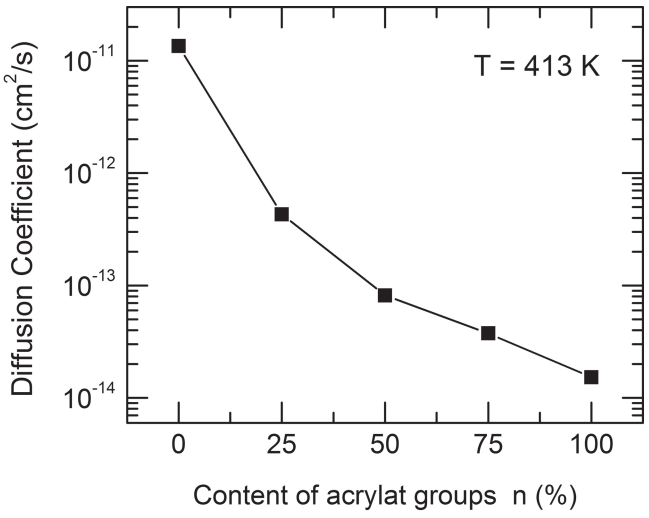

Figure 5. Diffusion coefficient of C_{60} as a function of the fraction of crosslinked polymer repeat units for PF2/6-A-n:m at 413 K.

sensor MEH-PPV film rather that by the time it takes to inject a C_{60} into the transport layer. This interpretation is supported by the fact that there is no deviation between the experimental and the theoretical arrival signal at long times. If the arriving C_{60} molecules would accumulate at the sensor interface rather than penetrate into, the arrival signal should feature an additional asymptotical tail because the thickness of the sensor layer is twice of the diffusion length of singlet excitons in MEH-PPV. Therefore a fraction of excitons should survive.

The above formalism clarifies the process of C_{60} through the polymer film but it is unnecessary for extracting values for the diffusion coefficient. It turns out that when operationally identifying the kink of the arrival signal from the intersection of the tangents prior and after the kink and using $D = L^2/(2t_{kink})$ (Equation 1) one obtains a D value that is virtually identical with that inferred from the "exact" treatment. This facilitates data analysis. The reason is that there are two opposing effects. On the one hand the kink time underestimates the arrival time because, in reality, it reflects only the arrival of the earliest C_{60} molecules but on the other hand one C_{60} molecule can quench all sensor excitons within the exciton capture radius which is 5–10 nm.[14]

From the temperature dependence of the arrival signal for thick PF2/6 films we calculated the diffusion coefficient for C_{60} in the PF2/6 layer. The data, shown in Figure 3b, bear out an activation energy of 0.65 +/− 0.05 eV. It is significantly lower than the activation inferred from the arrival signal for thin samples. Under the assumption that the activation energy indeed due to migration of C_{60} into the sensor layer we have to identify it with C_{60} diffusion within a MEH-PPV film.

We now explore the effect that crosslinking of poly mer chains has on C_{60} diffusion. Crosslinking has been accomplished via free radical polymerization of the acrylate groups. Figure 2 demonstrates that crosslinking 75% of the repeat units of polyfluorene (PF2/6-A-75:25) has a dramatic effect on i) the C_{60} arrival time as a function of the film thickness, ii) the associated activation energy, and iii) the trade-off between detachment of C_{60} from the C_{60} injection layer and subsequent diffusion. It is obvious that even in films as thin as 100–300 nm the C_{60} arrival time scales with the square of the film thickness. This indicates that C_{60} transport is in all cases diffusion limited rather than injection limited, and it allows calculating the diffusion coefficient. The data shown in **Figure 5** indicate that crosslinking 75% of the repeat units by acrylate linkages reduces the diffusion coefficient in a PF2/6 film at 393 K by a factor of 350. Upon complete crosslinking (PF2/6-A-100:0) C_{60} diffusion is retarded by a factor of 1000 as documented by Figure 5. The associated activation energy increases from 0.65 eV to 1.17 eV for the PF2/6-A-75:25 film. Obviously, crosslinking reduces the mobility of the polymer chains. By the way, when extrapolating the temperature dependence of $D(T)$ in the crosslinked sample down to 295 K one would arrive at a value of the diffusion coefficient as low as 4×10^{-19} cm^2 s^{-1} for PF2/6-A-75:25.

How does the value for the diffusion coefficient we obtain for the diffusion of C_{60} in PF2/6 compare to that of other molecule-in-polymer systems? Treat and coworkers used dynamic secondary ion mass spectroscopy to determine the diffusion coefficient for deuterated PCBM that was diffusing into a 265 nm layer of P3HT.[4] At 423 K, PCBM has travelled through the entire 265 nm layer after 30 s, thus yielding to a diffusion coefficient of $D = \frac{L^2}{2\tau} = \frac{(265\,\text{nm})^2}{2.30\text{s}} \approx 10^{-11}\,\text{cm}^2\,\text{s}^{-1}$, fully consistent with the value we obtained for 413 K for PF2/6 (c.f. Figure 3b). However while the values obtained for diffusion through the bulk are very similar for the two material systems the diffusion coefficient in P3HT is almost three orders of magnitude larger when lateral diffusion is measured.[3] It is conceivable in this case that PCBM transport is facilitated by hopping at the free surface of the polymer film.

Finally we will also extrapolate the experimental data to room temperature in order to make predictions regarding

unintentional doping of a polymer upon vapor deposition of a C_{60} layer. One may ask how long it takes until a 50 nm thick polymer film has been doped up to a concentration of 1% C_{60} per polymer repeat unit. Taking $N_0 = 10^{21}$ cm^{-3} as a rough estimate for the number density of repeat units, the number of C_{60} molecules in the 50 nm thick polymer film per unit area would then be 5×10^{13} cm^{-2}, that is, one half of the number of C_{60} molecules in a monolayer had to be incorporated into the film. As a rough estimate one identify the diffusion length of C_{60} with the film thickness. When extrapolating the diffusion coefficient to 293 K one arrives at $D(293\ \mathrm{K}) = 10^{-14}$ cm^2 s^{-1} and, from $\tau = L^2/2D$, a diffusion time of 1000 s. Obviously, a 50 nm thick PF2/6 film will contain a significant concentration of C_{60} in a sample held at room temperature already shortly after preparation. Crosslinking would prevent this effect because in a PF2/6-A-75–25 film the diffusion coefficient at room temperature is five orders of magnitude lower and the concomitant doping time would be by five orders of magnitude longer. Obviously, crosslinking is a way to prevent undesired C_{60} doping and for controlled device processing.

3. Conclusions

The present results demonstrate that the technique of fluorescence sensing provides a simple way to access the diffusion of C_{60} across a polymer film. It offers opportunity to study how modifications of the polymer structure changes molecular diffusion and thus opens new avenues for controlled processing of composite films. It can be applied to other polymers such as P3HT or low-bandgap polymers that are of more relevance to solar cell applications, provided that one can find a sufficiently red-shifted fluorescence probe that can be excited without simultaneously exciting the transport matrix.

4. Experimental Section

Sample Preparation: Samples for the diffusion experiment were prepared in a glove-box by first depositing a 15–17 nm thick MEH-PPV film onto a 2 cm × 2 cm quartz substrate from toluene solution by spin-coating. This thin film was annealed at 453 K for 10 min, which renders it resistant against swelling and/or dissolution when a subsequent transport layer is deposited onto it by spin coating. As transport layer, we used the polyfluorenes shown in Figure 2d, which were deposited onto the MEH-PPV by spin-coating from toluene solution to yield films ranging from 0.4 µm to 4.2 µm. Sample preparation is completed by vapor deposition of a 30 nm thick C_{60} layer with a shadow mask onto half of the polyfluorene film.

Materials: Poly(2-methoxy-5-(2-ethylhexyloxy)-1,4-phenylenevinylene) (MEH-PPV) was purchased by Aldrich and used as received. C_{60} was purchased by American Dye Source and also used as received. The polyfluorene polymers with photocrosslinkable acrylate units (Figure 1d) were prepared similar to the method described elsewhere.[15] They are crosslinked via free radical polymerization of the acrylate groups, leading to the formation of a polymer network (Figure 1e). In order to vary the degree of crosslinking a total of five derivatives are used in this work, labeled PF2/6-A-n:m, where *n* is the fraction of PF2/6 monomers with an acrylate group in the side chain and *m* is the fraction of non-crosslinkable PF2/6 monomers. We used PF2/6-A-100:0, PF2/6-A-75:25, PF2/6-A-50:50, PF2/6-A-25:75 and PF2/6-A-0:100, which is also referred to as PF2/6. The detailed procedure for the synthesis of the crosslinkable polyfluorenes is given in the supporting information. The crosslinking of the acrylate groups was carried out by photopolymerization using 1 wt% of the commercial photoinitiator Irgacure 784. Thin films of the polyfluorenes were irradiated at 40 °C for 10 min with a 50 W xenon lamp with UV filter.[15]

Experimental Setup: The MEH-PPV sensing layer is excited using a continuous-wave diode laser at 485 nm at an excitation density of 0.25 mW mm^{-2} and the photoluminescence is recorded using a fiber-coupled spectrometer connected to a CCD camera (Andor-Solis). For the measurement, the sample was held under vacuum in a heatable cryostat. To record each data point, the reference half and the C_{60}-covered half of the sample were excited immediately after each other, and shutters were used to limit the exposure time of the sample to the minimum.

Supporting Information

Supporting Information is available from the Wiley Online Library or from the author.

Acknowledgements

The authors acknowledge financial support by the Bavarian State Ministry of Science, Research, and the Arts through the Collaborative Research Network "Solar Technologies go Hybrid", by the German Science Foundation DFG through the doctoral training center GRK 1640 and helpful suggestions by an anonymous referee.

Received: April 10, 2014
Revised: June 10, 2014
Published online: August 8, 2014

[1] P. Westacott, J. R. Tumbleston, S. Shoaee, S. Fearn, J. H. Bannock, J. B. Gilchrist, S. Heutz, J. deMello, M. Heeney, H. Ade, J. Durrant, D. S. McPhail, N. Stingelin, *Energy Environ. Sci.* **2013**, *6*, 2756.
[2] G. J. Hedley, A. J. Ward, A. Alekseev, C. T. Howells, E. R. Martins, L. A. Serrano, G. Cooke, A. Ruseckas, I. D. W. Samuel, *Nat. Commun.* **2013**, 4.
[3] N. D. Treat, T. E. Mates, C. J. Hawker, E. J. Kramer, M. L. Chabinyc, *Macromolecules* **2013**, *46*, 1002.
[4] N. D. Treat, M. A. Brady, G. Smith, M. F. Toney, E. J. Kramer, C. J. Hawker, M. L. Chabinyc, *Adv. Energy Mater.* **2011**, *1*, 82.
[5] B. A. Collins, E. Gann, L. Guignard, X. He, C. R. McNeill, H. Ade, *J. Phys. Chem. Lett.* **2010**, *1*, 3160.
[6] O. V. Mikhnenko, H. Azimi, M. Scharber, M. Morana, P. W. M. Blom, M. A. Loi, *Energy Environ. Sci.* **2012**, *5*, 6960.
[7] C. Schwarz, H. Bässler, I. Bauer, J. M. Koenen, E. Preis, U. Scherf, A. Köhler, *Adv. Mater.* **2012**, *24*, 922.
[8] T. Cherdhirankorn, G. Floudas, H. J. Butt, K. Koynov, *Macromolecules* **2009**, *42*, 9183.
[9] H. Bässler, A. Köhler, *Top. Curr. Chem.* **2012**, *312*, 1.
[10] M. Pope, C. E. Swenberg, *Electronic Processes in Organic Crystals and Polymers*, Oxford University Press, Oxford **1999**.
[11] R. C. Powell, Z. G. Soos, *J. Lumin.* **1975**, *11*, 1.
[12] C. Im, J. M. Lupton, P. Schouwink, S. Heun, H. Becker, H. Bässler, *J. Chem. Phys.* **2002**, *117*, 1395.
[13] O. V. Mikhnenko, M. Kuik, J. Lin, N. van der Kaap, T. Q. Nguyen, P. W. M. Blom, *Adv. Mater.* **2014**, *26*, 1912.
[14] O. V. Mikhnenko, F. Cordella, A. B. Sieval, J. C. Hummelen, P. W. M. Blom, M. A. Loi, *J. Phys. Chem. B* **2008**, *112*, 11601.
[15] E. Scheler, P. Strohriegl, *Chem. Mater.* **2010**, *22*, 1410.